Title	Microwave bone imaging: experimental evaluation of calcaneus bone phantom and imaging prototype
Author(s)	Amin, Bilal; Sheridan, Colin; Kelly, Daniel; O'Halloran, Martin; Elahi, Muhammad Adnan
Publication Date	2020-12-14
Publication Information	Amin, Bilal, Sheridan, Colin, Kelly, Daniel, O'Halloran, Martin, & Elahi, Muhammad Adnan. (2020). Microwave bone imaging: experimental evaluation of calcaneus bone phantom and imaging prototype. Paper presented at the IEEE MTT-S International Microwave Biomedical Conference (IMBioC 2020), Toulouse, France, Virtual conference, 14-17 December.
Publisher	Institute of Electrical and Electronics Engineers
Link to publisher's version	https://dx.doi.org/10.1109/IMBIoC47321.2020.9385055
Item record	http://hdl.handle.net/10379/16711
DOI	http://dx.doi.org/10.1109/IMBIoC47321.2020.9385055

Microwave bone imaging: experimental evaluation of calcaneus bone phantom and imaging prototype

Bilal Amin
Electrical and Electronic Engineering
National University of Ireland Galway
Galway, Ireland
b.amin2@nuigalway.ie

Colin Sheridan
Electrical and Electronic Engineering
National University of Ireland Galway
Galway, Ireland
c.sheridan15@nuigalway.ie

Daniel Kelly
School of Medicine
National University of Ireland Galway
Galway, Ireland
d.kelly83@nuigalway.ie

Atif Shahzad
School of Medicine
National University of Ireland Galway
Galway, Ireland
atif.shahzad@nuigalway.ie

Martin O'Halloran
Electrical and Electronic Engineering
National University of Ireland Galway
Galway, Ireland
martin.ohalloran@nuigalway.ie

Muhammad Adnan Elahi
Electrical and Electronic Engineering
National University of Ireland Galway
Galway, Ireland
adnan.elahi@nuigalway.ie

***Abstract*—Microwave imaging (MWI) can be used as an alternate imaging modality for monitoring bone health. Evaluation and characterization of MWI prototype is a precursor step before *in vivo* investigation of bone dielectric properties. This paper presents experimental evaluation of a novel two layered simplified cylindrical shaped 3D printed human calcaneus bone phantom along with corresponding MWI prototype designed to image the bone phantom. The shape of the calcaneus bone was approximated with a cylinder. The external and internal layers represent cortical bone and trabecular bone respectively. Each layer of the phantom was filled with respective liquid tissue mimicking mixture (TMM). A MWI prototype was designed having six microstrip antennas in order to hold calcaneus bone phantom. The bone phantom was placed in the imaging prototype and scattered signals were measured at each antenna. Moreover, the performance of the system was explored by examining microwave measurement sensitivity. Based on the measured scattered signals the map of dielectric properties will be constructed by employing MWI algorithm and will be communicated in our future work. This two layered 3D printed human calcaneus bone phantom and imaging prototype can be used as a valuable test platform for pre-clinical assessment of calcaneus bone imaging for monitoring osteoporosis.**

Keywords—microwave imaging, calcaneus bone, dielectric properties, bone health, tissue mimicking mixtures

I. Introduction

The dielectric properties, namely relative permittivity (ε_r, unitless) and conductivity (σ, S/m) of biological tissues determine the transmission, absorption, and reflection of electromagnetic (EM) waves through human body [1]. The development of various EM diagnostic and therapeutic medical devices depends upon the knowledge of these properties [2]. MWI is a potential imaging modality for wide range of medical applications over the existing imaging modalities due to its key clinical advantages such as, portability, low cost, and non-ionizing radiations [3]. MWI has made significant development towards the diagnosis of breast cancer [4],[5],[6], brain stroke monitoring [7],[8], and cardiac imaging [9]. Beside these applications, recent studies have shown that MWI can be used to monitor osteoporosis [10],[11]. Osteoporosis is one of the major bone disease that results due to loss of minerals from bones and hence leads to bone fragility and fractures [3]. One of our earlier study has found a notable contrast between dielectric properties of healthy and diseased bone samples [12]. Therefore, this dielectric contrast can be exploited by using MWI. Current clinical practices widely employ Dual energy X-ray absorptiometry (DXA) scan for monitoring osteoporosis. But, due to standard X-ray doses, DXA scan poses long term health risks [13], therefore, a diagnostic device is required that does not use ionizing radiations.

Phantoms play vital role during the experimental evaluation and characterization of MWI prototype by providing realistic and controlled clinical scenario. Prior to *in vivo* dielectric properties assessment of target anatomical site, phantoms are used to model the dielectric properties of corresponding anatomical site [14]. Studies have shown that various TMMs exist that mimic the dielectric properties of various biological tissues [15]. Few of these TMMs are Oil-in-gelatin, Triton X-100, carbon-rubber mixtures, and glycerin [14]. One of our earlier study has presented Triton X-100 based TMMs to mimic the dielectric properties of cortical bone and trabecular bone

European Union's Horizon 2020 Programme/ERC Grant Agreement BioElecPro n. 637780.

separately [16]. However, to the best of authors' knowledge, no dedicated MWI prototype has ever been reported for bone imaging applications. In this study we have modelled human calcaneus bone with an equivalent simplified two layered 3D printed cylinder. The external layer of the cylinder represents the cortical bone, whereas, the inner layer represents the trabecular bone. A corresponding cylindrical shaped 3D printed phantom holder for MWI prototype was designed and antennas were mounted to acquire the microwave signals transmitted through the bone phantom. The proposed calcaneus bone phantom and corresponding MWI prototype is simplification of actual *in vivo* measurement scenario as the phantoms are not anatomically accurate. However, this two-layered phantom is reasonable approximation of the real calcaneus bone with each layer having approximately same volume as in the real calcaneus bone. This two layered 3D printed model and imaging prototype can be used as a tool for pre-clinical assessment of calcaneus bone imaging.

II. METHODOLOGY

The TMMs were composed of Triton X-100, water, and salt. The solution of these constituents was put in a glass beaker and was thoroughly mixed until the disappearance of air bubbles. Different concentrations of Triton X-100, water, and salt were tested in order to acquire the dielectric properties of target tissues. In this study, target tissues were cortical bone and trabecular bone.

The calcaneus bone resembles like an extended cylinder. A 3D modelling software Autodesk Fusion was used to produce a two layered cylindrical model of the human calcaneus bone. These two layers contained TMMs for cortical bone and trabecular bone. The dimensions of the inner and outer layer of the calcaneus bone model were designed to mimic the dimensions of the cortical bone and trabecular bone layers of the realistic calcaneus bone [17]. The calcaneus bone was chosen due to its similar composition of cortical bone to trabecular bone as found in the femoral head and lumbar spine [17],[18], which are main scanning sites for osteoporosis monitoring. To design imaging prototype, the cylindrical model was modified in Autodesk Fusion and six holes were created to place flexible microstrip antennas in direct contact with the cylindrical phantom. The antennas were placed equidistant from each other in order to keep the symmetry. These models were then printed at 200°C using a PLA filament. To prevent leakage of Triton X-100 solutions the thickness of walls was kept 2mm.

The imaging prototype was composed of 6 flexible microstrip antennas. The antennas were placed equidistant from each other in order to preserve the symmetry. The antennas were in direct contact with the calcaneus bone phantom. The height of imaging prototype was 82 mm whereas, the overall diameter was 54 mm. A 2-port ZNB40 Vector Network Analyzer and ZN-Z84 24-port switching matrix (Rohde and Schartz GmbH, Munich, Germany) collected microwave signals from antenna array. The signals were collected in a frequency range of 0.5-8.5 GHz. The input power of the VNA was set to 0 dBm.

III. RESULTS AND DISCUSSION

The external and internal layers of the 3D printed cylindrical bone phantom were filled with cortical bone and trabecular bone's TMM, respectively. The 3D printed cylindrical bone phantom is shown in Fig. 1(a). The bone phantom was placed in the imaging prototype shown in Fig. 1(b). The composition of Triton X-100, water, and salt for cortical bone was 77%, 23%, and 0.8 g/L respectively, whereas, for trabecular bone this composition was 69.5%, 30.5%, and 0.8 g/L respectively. The average percentage difference between proposed TMMs and reference data for cortical bone was found to be 9.6% for ε_r and 5% for σ, however for trabecular bone this difference was found less having numerical values of 3.4% for ε_r and 2.9% for σ. The proposed TMMs match the dispersive nature of the target tissues for the observed frequency range of 0.5-8.5 GHz. The dielectric properties of the TMMs display good agreement with Gabriel *et al*. [19]. The TMMs were constructed by using materials that have shown stable dielectric properties over time.

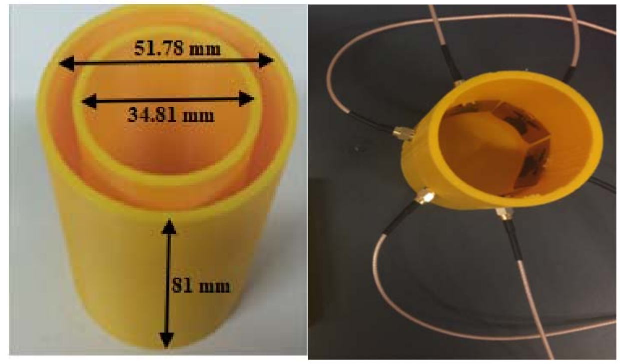

(a) (b)

Fig. 1. (a) Two layered calcaneus bone phantom (b) Imaging prototype

The measurement sensitivity is a key aspect for characterizing the system. Sensitivity can be defined as smallest signal that can be detected after subtraction of two set of measurements, i.e., measurement without target (WOT) and measurement with target (WT), i.e. the bone phantom in MWI prototype. To this end, we characterized the measurement sensitivity of our bone imaging prototype. Two set of measurements were performed. The first measurement was performed WOT, while, the second measurement was performed with WT. For both set of measurements a total of three measurements were averaged. A total of fifteen measurements were recorded. All the redundant data from reciprocal channels was not recorded and only unique measurements for each transmit-receive antenna pair were recorded. Similarly, the data from monostatic channels was not recorded as it includes the source field. Due to space limitations only the received signals for both set of measurements at antenna 10 when antenna 1 was transmitting are shown in Fig. 2 (a). The difference of signals for both set of measurements can be observed from Fig. 2 (b).

For an intermediate frequency (IF) of 1 kHz, the ZNB40 Vector Network Analyser provides a dynamic range of about 90 dB over 0.5 – 8.5 GHz frequency band. It can be observed from Fig. 2 (a) that the detected microwave signals are well above the sensitivity of measurement system. Similar trend was observed for measurements recorded for each transmit-receive antenna pair.

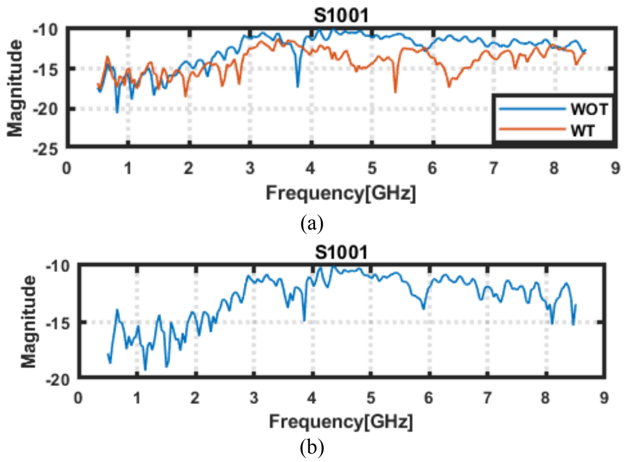

Fig. 2. (a) Received signal strength at antenna 10 when antenna 1 is transmitting for measurement WOT and measurement WT (b) Difference of two measurements

IV. Conclusion

In this study we have presented our initial findings towards experimental evaluation and characterization of MWI prototype designed to image simplified calcaneus bone phantom. The shape of human calcaneus bone was approximated with a simplified cylindrical model. A two layered 3D printed simplified cylindrical calcaneus bone phantom was presented along with its corresponding MWI prototype. The external and internal layers of cylindrical phantom were filled with liquid TMMs that mimic the dielectric properties of cortical bone and trabecular bone respectively. The TMMs were composed of Triton X-100, water, and salt. The calcaneus bone phantom was placed in the MWI prototype and microwave signals were recorded. The recorded signals were used to analyse the effect of bone phantom and sensitivity of measurement system. The future work leading to this study will be based on reconstruction of dielectric properties of bone phantom with the help of microwave tomography imaging (MTI) algorithm. Moreover, to replicate realistic *in vivo* scenario, the future study will consider a multi-layered phantom that will consider skin, muscle, and fat layers along with cortical bone and trabecular bone. The possible consequence of including these layers will result in reduced strength of microwave signals that will reach to trabecular bone, which is the main target tissue for evaluating bone health.

Two set of measurements were performed and the microwave signals were recorded across 0.5 - 8.5 GHz at an IF of 1kHz. A noticeable difference was observed in received signals for two set of measurements. Moreover, all the measured signals were found to be well within the dynamic range of system's measurement sensitivity for the observed frequency band of 0.5 - 8.5 GHz.

These initial measurements suggest that, this simplified two layered cylindrical shaped 3D printed structure along with corresponding MWI prototype will provide a feasible and realistic test platform for imaging purposes of calcaneus bone for monitoring bone health. These findings motivate towards the estimation of dielectric properties by employing MTI and hence the design and development of a MWI based device to measure *in vivo* dielectric properties of bone.

References

[1] S. Salahuddin, E. Porter, F. Krewer, and M. O' Halloran, "Optimised analytical models of the dielectric properties of biological tissue," *Med. Eng. Phys.*, vol. 43, pp. 103–111, 2017.

[2] B. Amin, M. A. Elahi, A. Shahzad, E. Porter, and M. O'Halloran, "A review of the dielectric properties of the bone for low frequency medical technologies," *Biomed. Phys. Eng. Express*, vol. 5, no. 2, p. 022001, 2019.

[3] B. Amin, M. A. Elahi, A. Shahzad, E. Porter, B. McDermott, and M. O'Halloran, "Dielectric properties of bones for the monitoring of osteoporosis," *Med. Biol. Eng. Comput.*, vol. 57, 2019.

[4] D. O'Loughlin, M. O'Halloran, B. M. Moloney, M. Glavin, E. Jones, and M. A. Elahi, "Microwave Breast Imaging: Clinical Advances and Remaining Challenges," *IEEE Trans. Biomed. Eng.*, vol. 65, no. 11, pp. 2580–2590, 2018.

[5] M. A. Elahi *et al.*, "Evaluation of image reconstruction algorithms for confocal microwave imaging: Application to patient data," *Sensors (Switzerland)*, vol. 18, no. 6, 2018.

[6] E. Porter, M. Coates, and M. Popović, "An Early Clinical Study of Time-Domain Microwave Radar for Breast Health Monitoring," *IEEE Trans. Biomed. Eng.*, vol. 63, no. 3, pp. 530–539, 2016.

[7] R. Scapaticci, M. Bjelogrlic, J. A. T. Vasquez, F. Vipiana, M. Mattes, and L. Crocco, "Microwave technology for brain imaging and monitoring: physical foundations, potential and limitations," in *Emerging Electromagnetic Technologies for Brain Diseases Diagnostics, Monitoring and Therapy*, Springer, 2018, pp. 7–35.

[8] R. Scapaticci, L. Di Donato, I. Catapano, and L. Crocco, "A feasibility study on microwave imaging for brain stroke monitoring," *Prog. Electromagn. Res.*, vol. 40I, pp. 305–324, 2012.

[9] S. Y. Semenov, A. E. Bulyshev, V. G. Posukh, Y. E. Sizov, T. C. Williams, and A. E. Souvorov, "Microwave tomography for detection/imaging of myocardial infarction. I. Excised canine hearts," *Ann. Biomed. Eng.*, vol. 31, no. 3, pp. 262–270, 2003.

[10] P. M. Meaney *et al.*, "Clinical microwave tomographic imaging of the calcaneus: A first-in-human case study of two subjects," *IEEE Trans. Biomed. Eng.*, vol. 59, no. 12, pp. 3304–3313, 2012.

[11] J. E. Fajardo, F. P. Lotto, F. Vericat, C. M. Carlevaro, and R. M. Irastorza, "Microwave tomography with phaseless data on the calcaneus by means of artificial neural networks," *Med. Biol. Eng. Comput.*, pp. 1–10, 2019.

[12] B. Amin *et al.*, "Dielectric characterization of diseased human trabecular bones at microwave frequency," *Med. Eng. Phys.*, pp. 1–8, 2020.

[13] A. H. Golnabi, P. M. Meaney, S. Geimer, T. Zhou, and K. D. Paulsen, "Microwave tomography for bone imaging," *Proc. - Int. Symp. Biomed. Imaging*, vol. 9, pp. 956–959, 2011.

[14] T. Rydholm, A. Fhager, M. Persson, S. Geimer, and P. Meaney, "Effects of the Plastic of the Realistic GeePS-L2S-Breast Phantom," *Diagnostics*, vol. 8, no. 3, p. 61, 2018.

[15] N. Joachimowicz, B. Duchêne, C. Conessa, and O. Meyer, "Anthropomorphic Breast and Head Phantoms for Microwave Imaging," *Diagnostics*, vol. 8, no. 4, p. 85, 2018.

[16] B. Amin, D. Kelly, A. Shahzad, M. O'Halloran, and M. A. Elahi, "Microwave calcaneus phantom for bone imaging applications," in *2020 14th European Conference on Antennas and Propagation (EuCAP)*, 2020, pp. 1–5.

[17] J. M. Vogel, R. D. Wasnich, and P. D. Ross, "The clinical relevance of calcaneus bone mineral measurements: a review," *Bone Miner.*, vol. 5, no. 1, pp. 35–58, 1988.

[18] B. Clarke, "Normal bone anatomy and physiology.," *Clin. J. Am. Soc. Nephrol.*, vol. 3 Suppl 3, no. Suppl 3, pp. 1–16, 2008.

[19] C. Gabriel *et al.*, "The dielectric properties of biological tissues : III . Parametric models for the dielectric spectrum of tissues The dielectric properties of biological tissues : III . Parametric models for the dielectric spectrum of tissues," 1996.